PREPRINT UCRL-78477

Conf-761108--29

# Lawrence Livermore Laboratory

## INTERFEROMETRIC MEASUREMENT OF LASER FUSION TARGETS

B. W. Weinstein and C. D. Hendricks

October 20, 1976

This paper was prepared for submission to the American Physical Society, 1976 Annual Meeting of the Division of Plasma Physics, November 15-19, 1976, San Francisco, California



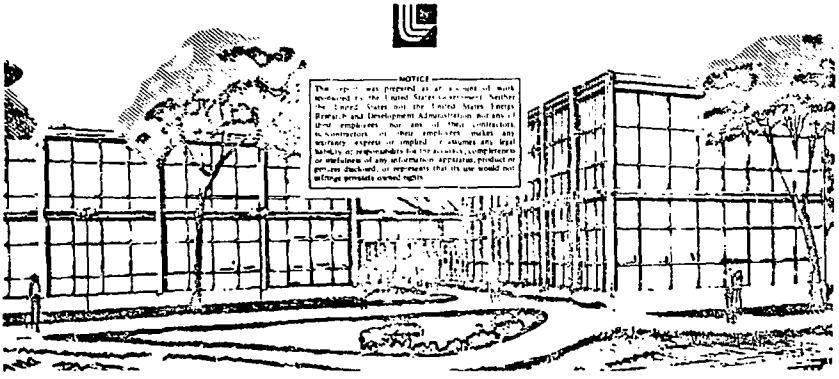

# INTERFEROMETRIC MEASUREMENT OF LASER FUSION TARGETS

B. W. Weinstein and C. D. Hendricks

University of California
Lawrence Livermore Laboratory
Livermore, California 94550

One of the important parameters of hollow glass microsphere laser fusion targets is the wall thickness and uniformity. We have shown previously how a combination of white light and monochromatic light interferometry can be used to measure the absolute optical path through the center of a glass microsphere.[1]

Here we will elaborate on the use of this technique to measure non-uniformities in microsphere walls. We will also discuss the way in which the actual optics used in the interferometer affect the wall thickness measurements.

## REVIEW OF MEASUREMENT METHOD

First a brief review of the basic thickness measurement technique. The interferometer which we use for these measurements is of the Twyman-Green type, which is a two-arm, double pass arrangement. The instrument is diagramed in Figure 1. With minor modifications, our analysis applies equally well to a single pass interferometer. For the double pass situation, the microballoon to be measured is placed on the surface of the reflecting mirror in one arm of the interferometer. If this mirror is slightly tilted with respect to the mirror in the reference arm of the interferometer then a white light illuminating source (which has a very short coherence length) can be used to find a reference point on the mirror to which the optical path is identical to the optical path through the microsphere. A monochromatic illumination source is then used to measure the optical path difference between this reference point and the point at which the microsphere is lying. This is a measure of the optical path through the microsphere.

Work performed under the auspices of the U.S. Energy Research & Development Administration under contract No. W-7405-Eng-48.

In terms of the number of fringes appearing between the reference point and the microsphere, the wall thickness is given by

$$t = x\lambda/4(n-1) \qquad (1)$$

where x is the number of fringes, $\lambda$ is the wavelength of the illumination and n is the index of refraction of the glass. If the microsphere contains a gas, the wall thickness formula becomes

$$t = \frac{1}{(n-1)} \left(\frac{x\lambda}{4} - r_i\ (n'-1)\right) \qquad (2)$$

where n' is the index of refraction of the gas and $r_i$ is the internal radius of the microsphere. One iteration to determine $r_i$ is usually adequate for a thin wall. (For a single pass interferometer, both of these expressions for t should be increased by a factor of 2.)

With the eye alone, one can estimate the phase shift caused by the microsphere to within about 1/10 of a fringe. If n = 1.5 and the wavelength of the monochromatic illuminating source is 0.54 μm (our typical values) then the measurement of the average of the top and bottom wall is accurate to about 0.03 μm (0.05 μm for single pass interferometry).

The above derivation assumes parallel illumination of the microsphere, and ignores any effects of the focusing optics used in illuminating and viewing the sphere. For the most common situations, where the wall of the microsphere is thin relative to the diameter of the ball, and the ball is illuminated and viewed with an objective of moderate magnification (10 x to 25 x) the errors introduced by this assumption are small—of the order of a few percent. We will discuss these errors and means of correcting for them later in this paper.

## MEASUREMENT OF WALL NONUNIFORMATIES

Before discussing the details of the interference process, we wish to give a simple explanation, on the same level as Equations (1) and (2), of how

one can measure defects in the microsphere walls with the interferometric process.

As with any technique which probes from only one direction, in order to measure defects one must have the capability of turning the microsphere while observing it so that defects on various parts of the ball become visible. Figure 2 illustrates this necessity for repositioning. Figure 2-a shows an interferometric picture of a microsphere which, aside from a small thick spot at about the 4 o'clock position, appears to be quite symmetric. Figure 2-b shows the same ball rolled 45° to the right. A serious asymmetry is now obvious.

It is imperative that one be able to measure, reposition, and remeasure so that one can build an accurate picture of defects which may not be visible in a specific orientation, or which require more than one view to unambiguously define them. This is particularly true when, as with hollow microspheres, the defects do not fit a simple model or pattern. One can always define some measure of nonuniformity, such as the maximum wall thickness excursion divided by the average wall thickness, but it is much more useful to determine the actual point-by-point topography. This is only possible when the ball can be viewed in any desired orientation.

One advantage of interferometry is that continuous viewing and repositioning is not difficult. We have found that a glass fiber pulled to a very fine tip ($\sim$ 1 μm) works very well for rolling a glass microsphere on a mirror surface. The fine tip keeps the ball from sticking to the fiber. For making measured rotations we hold the ball on a vacuum chuck and rotate the chuck holder.

After this aside on the necessity for a positioning capability, we now turn to the actual measurement of defects. If the mirror on which the ball lies is oriented parallel to the reference mirror, the defects appear as deviations from an otherwise symmetric pattern of circular fringes on the ball.

For defects of small spatial extent, the measurement procedure is very simple—one rotates the ball until the defect is against the mirror surface where the optics are focused and measures the change in optical path caused by the defect. The change in wall thickness is given by

$$\Delta t = \frac{\lambda \Delta x}{2(n-1)} \qquad (3)$$

where $\Delta x$ is the fringe shift caused by the defect.

For a defect such as the one seen in Figure 2, where the ball has a spherical outer surface and a spherical inner surface with their centers offset from one another, the fact that one measures through two opposing walls precludes measuring the defect at the center of the image. The proper orientation of the ball for making a measurement of a defect of this type is with the defect axis rotated by 45° as shown in Figure 2-b. Figure 3-a is a schematic diagram of the fringe pattern seen on the ball. Figure 3-b shows a cutaway of the ball in this position.

With the same technique used to measure the optical path through the center of the ball, one now measures the optical path through the points A, B, C, and C'. These points are located on a circle concentric with the circumference of the sphere, and points A and B are aligned with the thickest and thinest parts of the wall. By simply comparing the ratios of the optical paths at these points one can find the magnitude of the defect without the necessity for a detailed calculation of what the optical path should be at each point on the ball.

That one can characterize the defect by simply comparing the ratios of the optical paths at the different points is obvious if one notes that the presence of the defect does not significantly change the geometry of the path which a light ray takes through the balloon. For example, in a microsphere with a 50 μm radius and a 1 μm average wall which has a spherical inner surface displaced by 0.2 μm from a spherical outer surface, a ray follows a path with a

maximum deviation of only a few miliradians from the path of a ray through a perfect microsphere. Thus to first order the only differences in the optical paths through points A and B and those through points C and C' in Figure 3 are caused by the increase or decrease in optical path through the defect and not by any difference in the geometry of the path taken by the ray through the ball.

The fractional increase in the thickness of the lower wall at point A is

$$\frac{\Delta t_A}{\bar{t}} = \frac{(P_A - P_B)}{P_C} \qquad (4)$$

where $\bar{t}$ is the average wall thickness as measured at the center of the microsphere, and $P_A$, $P_B$, and $P_C$ are the optical paths through points A, B, and C respectively. (The average of $P_A$ and $P_B$ can be used instead of a measurement at point C. This reduces the number of measurements and therefore reduces the error somewhat.)

The eye is very good at detecting the non-concentricity of a fringe and the outside of the ball, and one can detect the existence of defects which cause a shift in optical path of 1/10 of a fringe. For glass with a refractive index of 1.5, this implies a sensitivity of about 0.05 μm.

The overall accuracy in measuring a more severe defect of this type is reduced somewhat by the fact that the measurement of the defect must be made at an off-center point. In practice the way one makes the measurement is by adjusting the interferometer so that a fringe is located at point A, readjusting so that the fringe is located at point B, and measuring the difference in optical path. The accuracy with which one can locate the fringe at the points A and B is determined by the resolution of the microscope.

From curves of optical path as a function of position on the ball calculated for parallel light illumination by Stone et al[2] we can calculate the effect on the defect measurement of the uncertainty in positioning the fringe. We find that on a 100 μm diameter, 1 μm thick, hollow microsphere; at a point 0.7

(sine 45°) of the way from the center to the edge; the derivation of the optical path with respect to position on the ball is about 0.04 μm/μm. If we have an uncertainty of 2 μm in the positioning of the fringe, an error of 0.08 μm occurs in the measurement of $P_A - P_B$. From Equation 3 we see that this results in an error of 0.03 μm in the measurement of the thickness of the defect.

With a combination of the off center measurement technique just described, and on center measurements of defects where appropriate, one can characterize any defect in a microsphere without having to resort to a detailed calculation of the ray paths.

## EFFECT OF MICROSCOPE OPTICS ON INTERFEROMETRIC MEASUREMENTS

We will next turn to a more careful consideration of the interference phenomenon and examine the effect of the microscope illumination and viewing systems. We will find that for thin-walled microspheres the simple analysis given above is entirely adequate as long as a microscope objective with numerical aperture less than about 0.3 (acceptance angle less than about 20° is used. Systems with a larger numerical aperture can be used if the illumination is apertured to a cone with a small half-angle.

## MICROBALLOON RAY TRACE

To analyze the effect of the optical system, one must trace rays from various parts of the system through the microsphere. For a uniform hollow sphere this is not particularly complicated. The procedure is illustrated by Figure 4. The first thing to note is that the ray trace is symmetric about a line through the center of the ball and perpendicular to the ray path. Thus the angles at the exit wall are the same as the angles at the wall where the ray is incident.

The only parameters are the 3 indices of refraction (the surrounding medium, the wall, and the interior of the ball—$n_0$, $n_1$ and $n_2$ respectively); the ratio

of the wall thickness t to the inner radius $r_i$, and the angle of incidence of the ray on the surface, $\theta_{I1}$.

The relationships of the angles shown in Figure 4 are:

$$\theta_1 = \sin^{-1} \left(\frac{n_0}{n_1} \sin\theta_{I1}\right) \tag{5}$$

$$\Delta = \sin^{-1} \left[\frac{t}{r_i} \frac{1}{\cot \theta_1 - \tan (\Delta/2)}\right] \tag{6}$$

$$\theta_2 = \sin^{-1} \left[ \frac{n_1}{n_2} \sin (\theta_1 + \Delta) \right] \tag{7}$$

$$\theta_T = \pi + 2\theta_2 - 2\Delta \tag{8}$$

The only complication is that we must iterate Equation 5 to obtain $\Delta$, but this generally converges rapidly since tan $(\Delta/2)$ is ordinarily much smaller than cot $\theta_1$. In terms of these angles, the total optical path through the ball from entrance point to exit point is

$$\Delta P_1 = 2 r_i \left(n_1 \frac{\sin \Delta}{\sin \theta_1} + \cos \theta_2\right) . \tag{9}$$

For a given microsphere, the only variables are the position that the ray strikes the ball and the angle of incidence. It is simplest to give the position of incidence as an angular coordinate $\psi_{I1}$ measured from the top of the ball. The exit point $\psi_{E1}$ is then simply

$$\psi_{E1} = \psi_{I1} + \theta_T . \tag{10}$$

The exit angle of the ray (the angle between the exiting ray and the normal at $\psi_{E1}$) is simply $-\theta_{I1}$.

For tracing rays in an arm of the reflection interferometer, (Figure 1) a little more geometrical bookkeeping is necessary to compute the path as the ray bounces from the mirror and to keep track of the total optical path length for a given ray. The geometry of the bounce is shown in Figure 5. The position at which the ray reenters the ball, $\psi_{I2}$, and the new angle of incidence $\theta_{I2}$ are found to be

$$\psi_{I2} = \pi + \gamma \tag{11}$$

$$\theta_{I2} = \phi + \gamma \tag{12}$$

where

$$\gamma = \sin^{-1} [t \cos \phi - \sin \phi \, (1-t^2)^{1/2}]$$

with

$$t \equiv 2 \sin \phi + \sin \theta_I$$

and

$$\phi = \psi_{E1} - \pi - \theta_{I1} .$$

The total length of the path between exiting and reentering the ball is

$$\Delta P_2 = \frac{n_o \, r_o}{\cos \phi} (2 + \cos \psi_{E1} + \cos \psi_{I2}) \tag{13}$$

where $r_o$ is the outer radius of the ball. (Note that $\cos \psi_{E1}$ and $\cos \psi_{I2}$ are both negative.)

The trace back trough the microsphere is of course carried out exactly like the initial trace through.

Once the geometry has been done, the actual tracing of a ray through a ball is simple enough that it can be programmed on a hand-held calculator. One can calculate the path of any given ray and also its phase relative to the rays in the other arm of the interferometer with which it eventually interfers. At any point in the field of view, one can thereby find the phase difference between the two arms of the interferometer caused by the presence of the glass microsphere.

## RESULTS OF RAY TRACE CALCULATIONS FOR NON PARALLEL ILLUMINATION

Several earlier papers have treated aspects of the interference pattern seen on hollow glass microspheres by assuming parallel incident illumination.[2,3,4] We have examined the situation without making this assumption, and find that under conditions of high magnification the results are altered significantly.

If the microsphere is illuminated by parallel light, then the rays which appear to come from a given point in the focal plane of the system must have traversed one specific path through the ball. With the Twyman-Green system, however, the illumination comes from light which is parallel in the interior of the interferometer and is focused by the final objectives. Each point in the field of view is illuminated by a cone of light with a half angle determined by the numerical aperture of the objective lens and by the details of the illumination system being used. Also, all light propagating from the sample back towards the lens along a path which lies in the acceptance cone of the objective is captured and focused in the image plane. Thus the light which appears at any particular point in the image plane is the sum of many rays which have taken different paths through the microsphere.

There are two undesirable effects of the multiple paths. First, it is obvious that at the center of the image of the microsphere the information is not exclusively about the projection of the center of the microsphere onto the mirror. Secondly, two rays which appear at the same point in the image plane have not necessarily traversed the same optical distance and so may no longer be in phase.

We will first address the aspect of the overlap of information from different points on the ball. Clearly, the pattern in the image plane contains some sort of "average" over the upper surface of the ball, and the spatial extent of this averaging is controlled by the numerical aperture of the objective. (This is really nothing more than a statement of the fact that we look through an upper wall which is out of focus.) A more subtle problem is that the information at the center of the image is not even exclusively from the center of the bottom wall of the microsphere.

The fact that the measurement is an average over a portion of the upper surface is not usually a problem, and is often actually an advantage. For example, a (spatially) small defect on the upper surface gets "averaged out" and has a very minor effect on the measurement of defects on the lower surface.

The averaging does cause an error in the measurement of the defect shown in Figures 2 and 3, since in the measurement of the optical path at point B in Figure 3 one is actually measuring an average over an area around the thin part of the microsphere. If the numerical aperture of the objective is small, or if the illumination is confined to a narrow cone, then the error introduced by the out-of-focus upper surface is small. For example if the illumination/acceptance angle is $\pm$ 10°, the error in measuring the defect is only about 2%.

Figure 6 shows the extent of the overlap of information from points on the lower surface of the ball. The amount of overlap (expressed in terms of an angular fraction of the ball) is plotted as a function of the smaller of the objective aperture angle and the illumination angle. Curves for three values of $t/r_o$ are shown.

If the objective acceptance angle is large enough to allow more overlap than the desired resolution, one must aperture the illumination system to give a small enough illumination angle to assure the desired level of resolution.

We next turn our attention to the variation in the length of the different optical paths taken by rays which appear at the same point in the image. Our ray trace results show that at each point of the image, the ray with the longest

optical path to the image plane is the ray which was incident on the ball parallel to the optic axis. All other rays appearing at that point in the image followed shorter paths. The variation in ray path through the microsphere is shown in Figure 7 as a function of the angle between the optic axis and the final path of the ray after it exits the microsphere. The normalization is to the ray with the longest optical path which appears at the point of interest in the image plane. This normalization length is therefore just the optical path which one would calculate assuming parallel illumination.[2,3,4]

For the center of the microsphere image and an illumination and acceptance angle of $\pm$ 10°, (typical for about a 10 x objective), the spread in optical path lengths is only about 1%. With an acceptance and illumination angle of $\pm$ 40° (typical for a 60 x objective), the total variation is about 10%. These values are more or less independent of $t/r_o$.

It is easy to have a situation where the total phase spread of the light is large enough to reduce the coherence to the point that interference measurements are not possible. This will occur when the total phase spread is on the order of $\pi$. For a $\pm$ 10° acceptance angle this would occur for a ball wall about 10 μm thick. For a $\pm$ 20° angle (about 25 x) it would occur for a wall thickness of only 2.5 μm. A fully illuminated objective with a $\pm$ 40° acceptance angle would lose coherence at a wall thickness of only 1 μm. Noticeable degradation in the coherence of the light will take place for even thinner walls. It is obvious that proper aperturing of the illumination is necessary except for thin balls or a small numerical aperture objective lens.

A related problem is that what one actually measures is an average optical path. For most measurements, aperturing to insure good coherence will also insure a sufficiently accurate absolute value for the measurement. If very high absolute accuracy is desired, one can use an integral of the calculated path length differences to correct for the effect of the multiple-path illumination.

## CONCLUSIONS

Quantitative interferometric characterization of the wall thickness variations of hollow glass microspheres is straight forward. Comparing the ratios of the optical paths at geometrically equivalent points circumvents the need for detailed calculations of the expected optical path at a given point on the microsphere.

If both a large illumination angle and a large aperture acceptance angle are used, the multiple paths of light rays through the ball causes degradation in both the spatial and the phase resolution of the interferometer. These problems can be overcome by proper aperturing of the illumination.

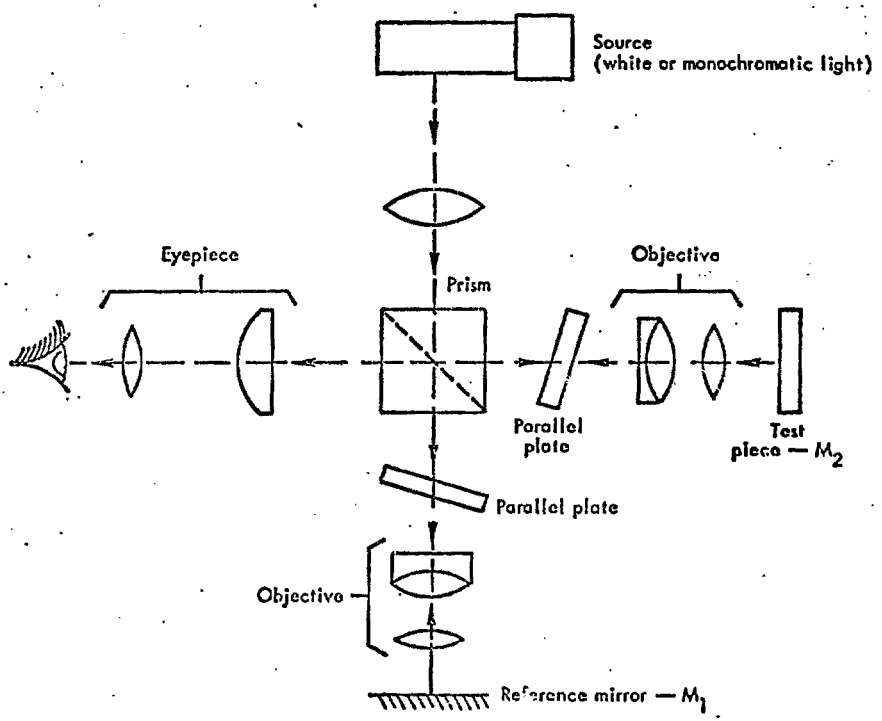
Source
(white or monochromatic light)
Eyepiece
Prism
Objective
Parallel
plate
Test
piece — $M_2$
Parallel plate
Objective
Reference mirror — $M_1$

Fig 1

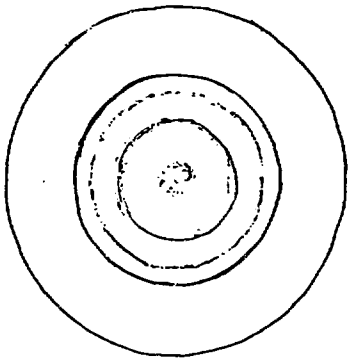

(a)

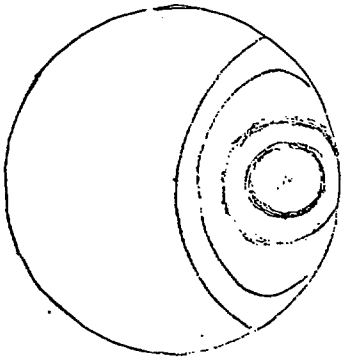

(b)

Fig. 2

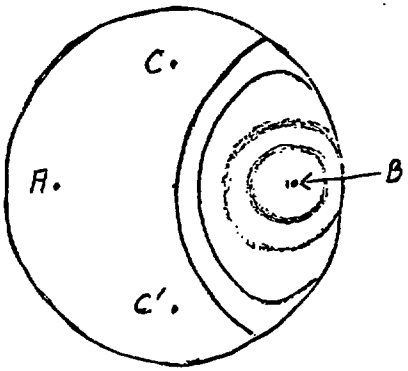


(a)

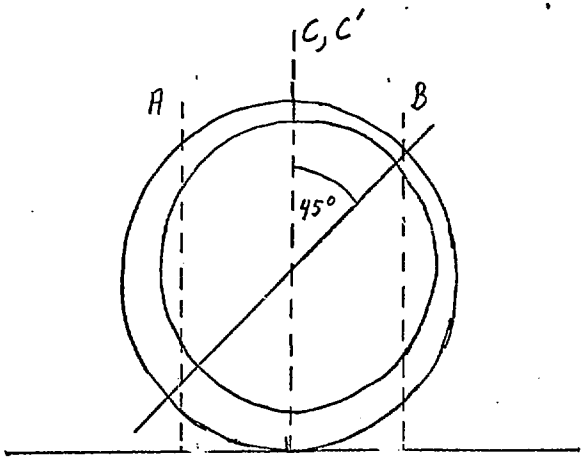


(b)

Fig.

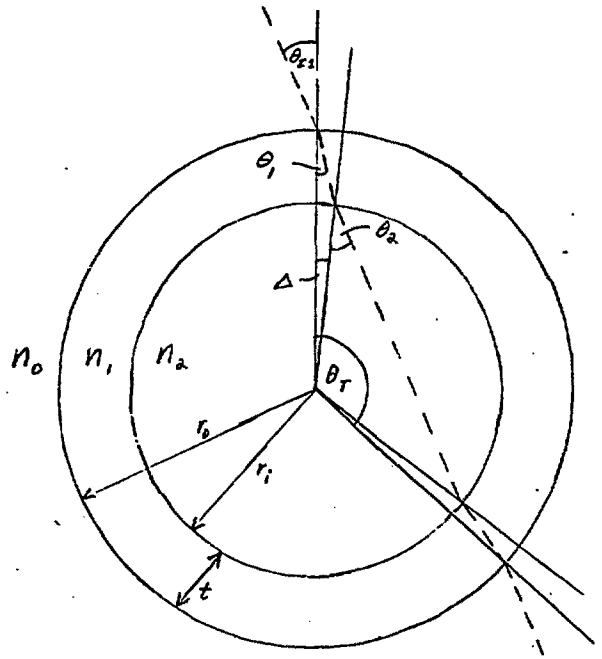


$$\theta_1 = \sin^{-1}\left(\frac{n_0}{n_1}\sin\theta_0\right)$$

$$\Delta = \sin^{-1}\left[\frac{t}{r_i}\cdot\frac{1}{\cot\theta_2 - \tan(\theta/2)}\right]$$

$$\theta_2 = \sin^{-1}\left[\frac{n_1}{n_2}\sin(\theta_1+\Delta)\right]$$

$$\theta_T = 2\left(90+\theta_2-\Delta\right)$$

$$P_1 = 2r_i\left(n_1\frac{\sin\Delta}{\sin\theta_1} + n_2\cos\theta_2\right)$$

Fig. 4

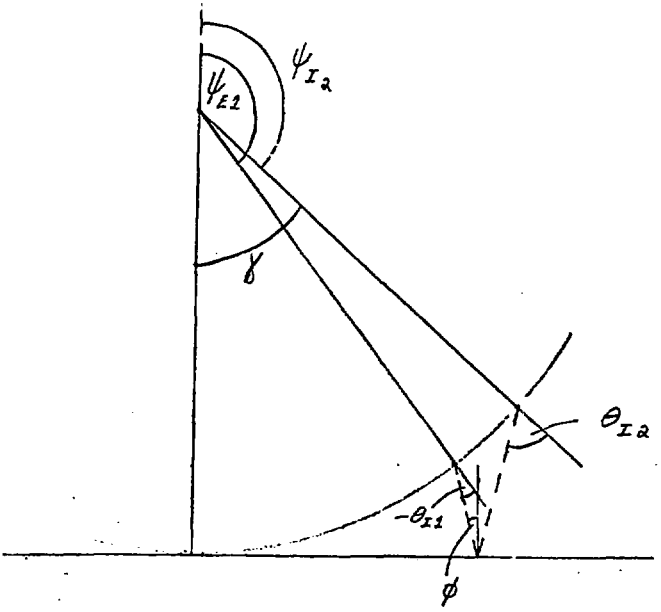


$$\psi_{I2} = \pi + \gamma \; ; \quad \theta_{I2} = \phi + \gamma$$

$$\gamma = \sin^{-1}\left( t\cos\phi - \sin\phi\sqrt{1-t^2} \right)$$

$$t \equiv 2\sin\phi + \sin\theta$$

$$\phi = \psi_{E1} - \theta_{I1} - \pi$$

$$\rho_2 = \frac{r_0}{\cos\phi}\left(2 + \cos\psi_{E1} + \cos\psi_{I2}\right).$$

Fig 5

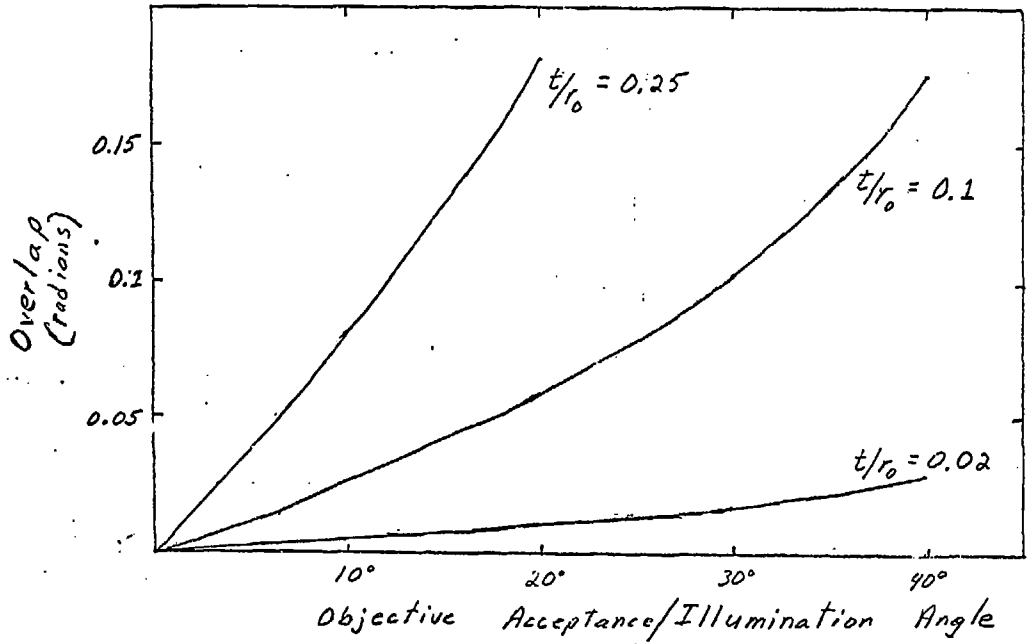
$t/r_0 = 0.25$
$t/r_0 = 0.1$
$t/r_0 = 0.02$
0.15
0.1
0.05
Overlap (radians)
10°
20°
30°
40°
Objective Acceptance/Illumination Angle

Fig. 6

Fig. 7